ЯДЕРНА ФІЗИКА
NUCLEAR PHYSICS

УДК 539.121.7, 52-852 https://doi.org/10.15407/jnpae2024.04.341

I. F. Hussein[1,*], A. A. Al-Rubaiee[1], A. F. Mkhaiber[2]

[1] *Mustansiriyah University, College of Science, Department of Physics, Baghdad, Iraq*
[2] *University of Baghdad, Department of Physics, College of Education for Pure Sciences, Baghdad, Iraq*

*Corresponding author: itabfadhil@uomustansiriyah.edu.iq

MEAN ARRIVAL TIME DISTRIBUTIONS OF EXTENSIVE AIR SHOWERS AT ULTRAHIGH ENERGIES

This paper investigates extensive air showers by estimating the muon and electron mean arrival time distributions at ultrahigh energies for various cosmic-ray particles. The Monte Carlo package AIRES (version 19.04.00) was used to perform simulations at energies of 10^{19} and 10^{20} eV. The influence of primary particles (p, ^{56}Fe, and ^{16}O), energies, and zenith angles (0°, 10°, and 20°) on the mean arrival time of muonic and electromagnetic shower disks created in an extensive air shower was examined. Parameterized mean arrival time distributions were calculated for secondary particles e^-, e^+, and μ, created by proton, iron, and oxygen nuclei at energy 10^{19} eV in a vertical shower. A polynomial function for these primaries in vertical showers was established using the results of this simulation. The results were compared with the KASCADE-Grande experiment and Sciutto's simulations at energy 10^{20} eV and θ = 0. In this work the construction of a database that can be used to compute the arrival time of elementary particles is crucial in ultra-high energy ranges through an analytic description between the time structure and the distance distribution.

Keywords: mean arrival time distribution, extensive air shower, AIRES, electromagnetic shower simulations.

1. Introduction

Cosmic rays (CRs) entering the atmosphere collide with the nuclei of air molecules, creating secondary particles that contribute to the development of extensive air showers (EAS). Three primary components are shown: electromagnetic (e^+, e^-, and γ), muonic (μ^+ and μ^-), and hadronic (mainly $\pi^\pm$, π^o, n, p, $K^\pm$, and K^o). Electromagnetic particles are the most common, accounting for 98 % of total energy, with the balance shared by the other components (the muonic component accounting for 1.7 %). It is difficult to analyze EAS at the highest energies because the environment forms part of the detector, requiring the interpretation of indirect measurements. An EAS is a complex series of interactions with relatively high particle numbers for which only limited data samples have been collected. From these samples, the primary particle's characteristics can be determined using either simplified models or intricate numerical simulations [1, 2].

Muons are necessarily highly energetic when they reach the ground; if this were not the case, they would have decayed during their trip. As a result of their long radiation lengths, they undergo few interactions along their paths from their points of origin to the ground. Consequently, if muons are detected in the signal, it can be concluded that the signal is from the early portion of the shower front, which is often used to determine the mean arrival time to be employed in the direction reconstruction [3]. Moreover, muons have a significantly thinner lateral distribution than electrons, which always dominate ground-level signals sufficiently far from the shower axis. Therefore, it is critical to gain a better understanding of this time structure in this framework. Additionally, faster simulation tools could be developed based on this information and, for specific parameterizations, may be useful for analysis and the creation of improved detectors [4].

When considering a complete shower simulation, the front time structure depends strongly on the specific details of particle transport mechanisms. A valuable analysis of the time structure of EAS at very high energies using the AIRES code has been given in [5, 6]. These EASs may be determined by collecting samples of the particle shower disk at ground level using detector arrays; quantifying the number of muons is essential for reconstructing the energy and identifying of primary particle [7].

Muons and electrons arrive at observation levels at different times because of the further growth of the EAS's muonic and electromagnetic components. Muons are typically formed at a higher altitude than electrons, and they scatter significantly less. When the radial distance of the shower core increases, this disparity in arrival time rises. Numerous studies, such as Pierre Auger Observatory (PAO) [8, 9] KASCADE (Karlsruhe Shower Core and Array Detector) [10, 11], GREX/COVER PLASTEX [12], and AKENO [13, 14], have explored the distributions of particle arrival times but have been limited to small core distances. This research extends their conclusions on the discrepancies in mean arrival time of the muonic and electronic EAS components to distances range 0 - 1500 m further from the center of the shower, for vertical and inclined showers with distinct primary particles.

2. Mean arrival time profile

Most particles in the shower disk are characterized by the general temporal aspects of the air showers, specifically the electromagnetic particles and the muons. A shower appears to an observer as a disk of particles with a specific thickness that spreads in the atmosphere along the shower axis at the speed of light. Fig. 1 shows a cutaway view of the situation at the vertical plane with a shower axis just before the shower hits the ground [15].

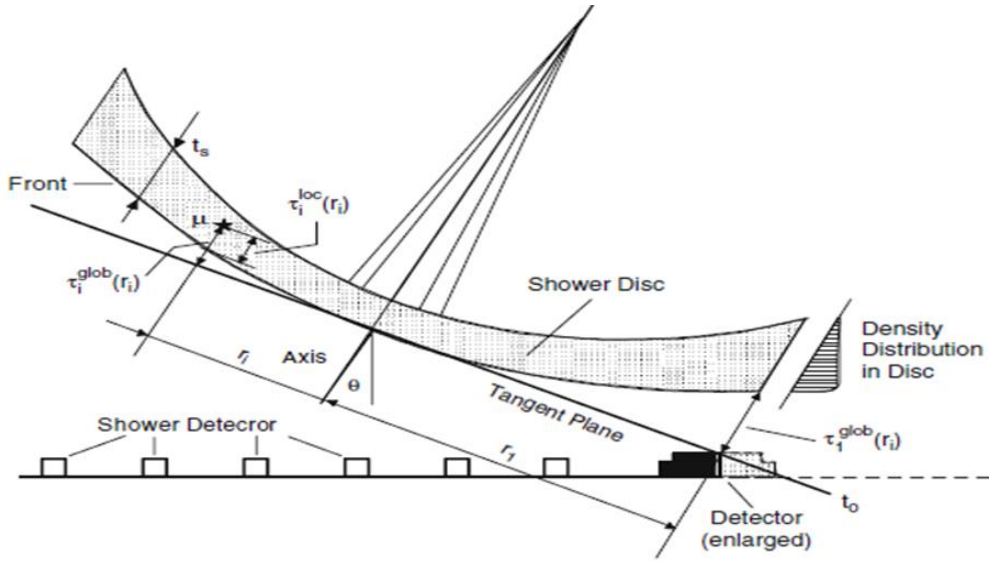

Fig. 1. Schematic illustrating the development of showers in the atmosphere [15].

The shower disk expands radially as the photon and particle density decrease. The thickness of the shower disk is finite due to two factors resulting in the time dispersion of photons and particles. First, the particles have a range of Lorentz factors depending on their energies. Second, there are differences in the path lengths of the particles' and photons' trajectories, which are brought about by multiple scattering processes (e.g., interactions, Coulomb scattering, and transverse momenta) and geomagnetic deflection, which play an important role in lateral dispersion of photons and particles distant from the axis of shower's [16].

In general, the mean arrival time $t_i(r_i)$ of a particle (i) at a distance (r_i) from the axis of the showers is given relative to an empirically determined reference time t_0, which is typically defined as the arrival time of the shower core's leading edge $r=0$; this establishes the position known as the tangent plane, which is orthogonal to the axis of the showers. The mean arrival time of particle $t_i(r_i)$, which is stated in terms of the time of arrival of the tangent plane t_0, in terms of delay in time $\tau_i(r_i)$, within related to that plane. This time is frequently used to describe the global time $\tau_i^{glob}(r_i)$ [17]

$$\tau_i^{glob}(r_i)=\tau_i(r_i)-t_0(r=0). \quad (1)$$

The time delay $\tau_i^{loc}(r_i)$ is determined according to the local reference time $t_0^{loc}(r_i)$, concerning a curved shower enclosure's front face at r_i, then

$$\tau_i^{loc}(r_i)=\tau_i(r_i)-t_0^{loc}(r_i). \quad (2)$$

In practice, the reference time equals zero and is established by the arrival of the first particle of the shower t_1 at the detector situated at a distance r_1 from a shower. Consequently,

$$\tau_1^{glob}(r_1)=t_1(r_1)-t_0(r=0). \quad (3)$$

In simulations, a fictional spherical light front is formed with the point of primary's first impact with an atmosphere and travels throughout space at light speed. It monitors the time of all simulation particles throughout the shower [17, 18].

The average delay in time at various distances from the core r in the event is

$$\tau r=\left(\frac{1}{N}\right)\sum_{i=1}^{N}\tau_i, \quad (4)$$

where N is the total number of particles in the distribution, the observable τr is a space-time profile of shower disks [19].

3. Simulation of mean arrival time using AIRES

AIRES is an abbreviation for AIR-shower extended simulations, which refers to the collection

of programs and subroutines that can be used to simulate EAS particles formed as a result of the interaction at high-energy main CRs with the environment and to govern all associated particles within output data [20, 21]. AIRES models the whole space-time particle propagation in a realistic environment that incorporates atmospheric properties, Earth curvature, and the Earth's magnetic field. When the number of the particles in showers is excessively large, the statistical sample selection (named thinning) is used. AIRES's thinning algorithms are equitable, in that statistical samples never alter the average values of the output observables. Various particles are considered in the AIRES simulations, including gammas, electrons, positrons, muons, mesons, pions, nucleons, antinucleons, lambda baryons, and nuclei up to Z = 36. A primary particle in an EAS may be a proton, an iron nucleus, or any of the previously mentioned particles (e^-, e^+, μ^-, μ^+, π^-, π^+), with energy ranging from about 10^9 eV up to about 10^{21} eV [22]. The present work used the information of the surface detector (SD) of the PAO which includes ground level (1400 m above the sea level) with slant depth 1000 g/cm^2, cut energies for gamma, electrons, muons and meson are 80 keV, 80 keV, 10 MeV, and 60 MeV, respectively, 18 EAS were simulated using the Monte Carlo program AIRES version (19.04.00) using QGSJetII.04 interaction models for high-energy hadronic collisions [23]. Three atomic nuclei were considered: proton, iron, and oxygen, with energies of 10^{19} and 10^{20} eV and zenith angles of 0°, 10°, and 20°. Also, the energy of the thinning algorithm was set to ($\epsilon_{th} = 10^{-6}$), the mean arrival time simulations accounted for various particles, including electrons, positrons, and muons, created in the EAS.

4. Results and discussion

Fig. 2 shows the simulated mean arrival times of e^-, e^+, and μ as a function of R, which is the distance from intersection of the shower axis with the Earth's surface, produced using AIRES for three primary particles (iron, oxygen nuclei, and protons) and energies 10^{19} and 10^{20} eV. In hadronic showers, the primary distinction is the presence of a slow electromagnetic component that becomes increasingly noticeable at significant distances from the shower center.

The statistical uncertainties are shown as the error bars, propagating the correlation between the arrival time of electronic and muonic showers with R(m), and the systematic uncertainty can be shown by SD.

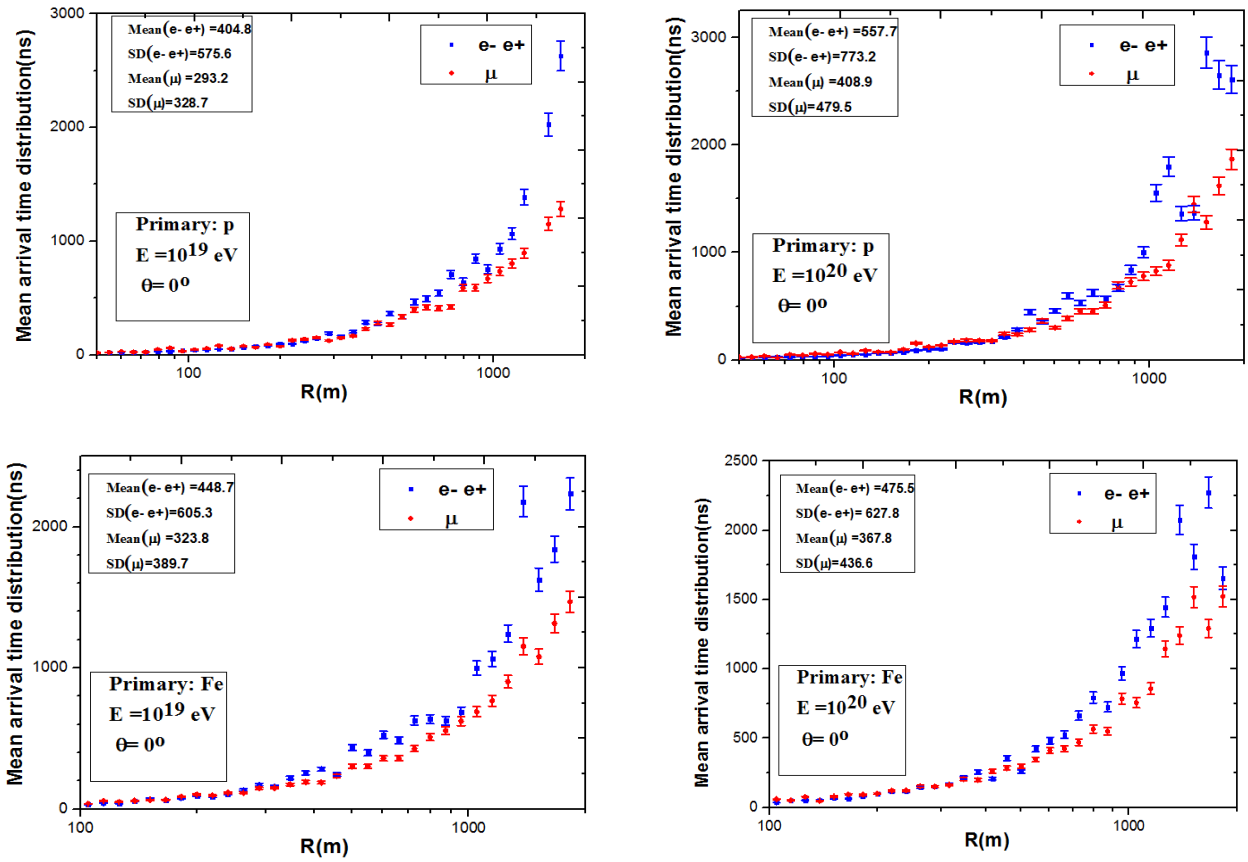

Continuation of Fig. 2

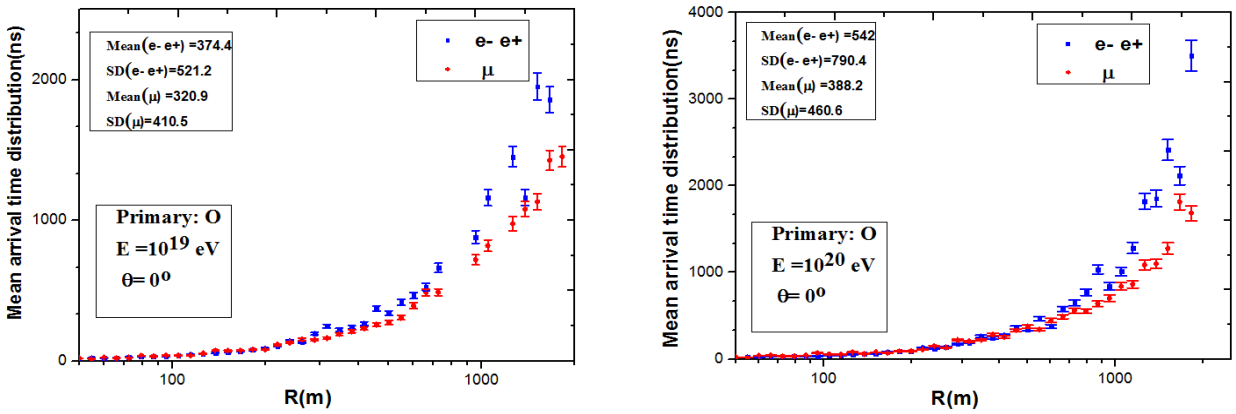

Fig. 2. Mean arrival time distribution of e^-, e^+, and μ as a function of distance from a core vertical shower for various primary particles and energies. (See color Figure on the journal website.)

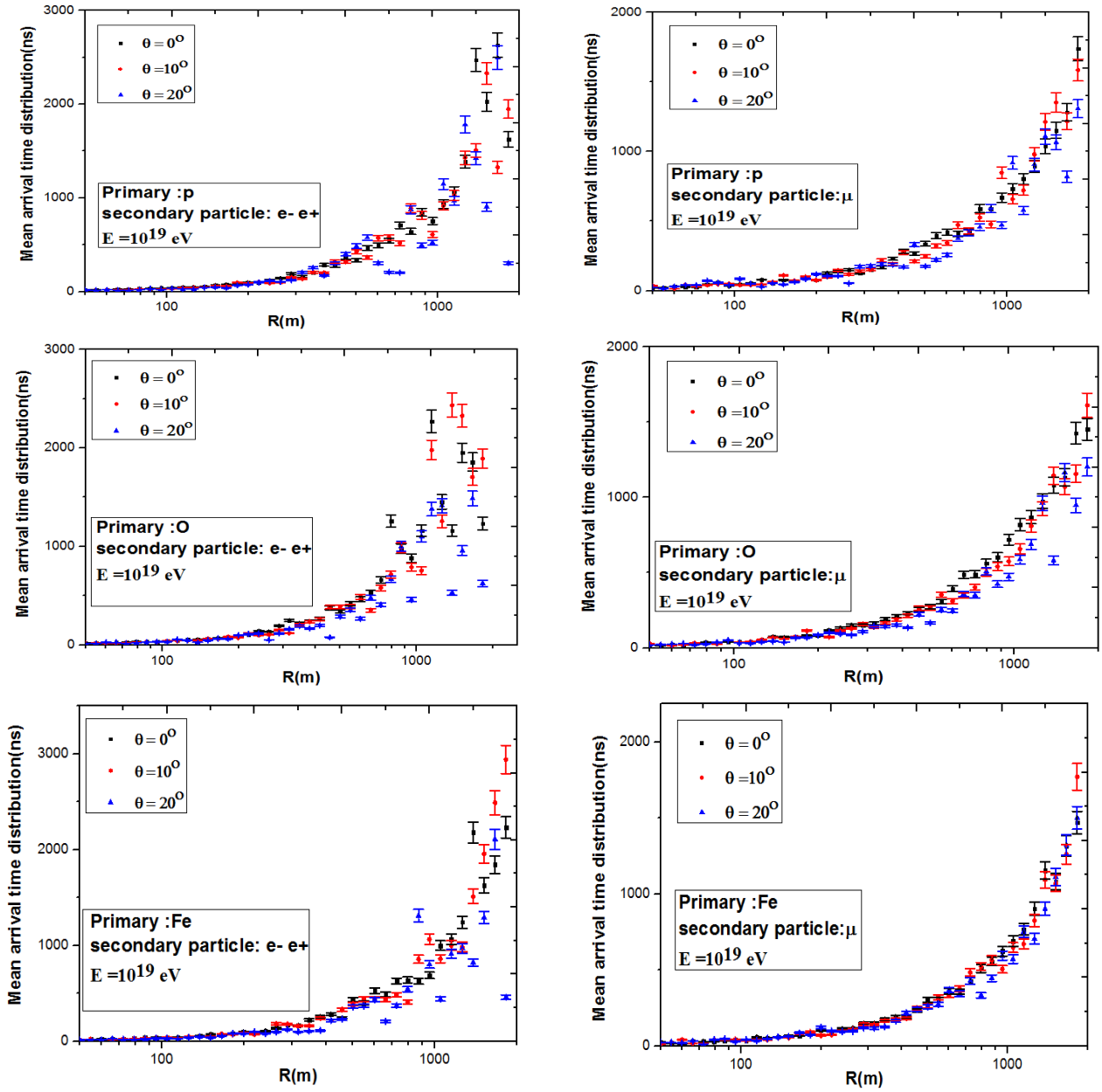

Fig. 3. Mean arrival time of e^-, e^+, and μ as a function of the distance from the core shower for various primary particles and energies for θ = 0°, θ = 10°, and θ = 20°, the statistical uncertainties are shown by error bars. (See color Figure on the journal website.)

For each simulated EAS event, a number of EAS observables have been reconstructed: the electromagnetic shower size, the muon content, the shower age, and in particular the temporal parameters of muon arrival time distributions and their changes with distance from the shower axis. It can be observed that at $R = 500$ m, the total shower variance (which is unity for the normalized residuals at all core distances and zenith angles) may be completely explained by sampling fluctuations. However, sample variations are inadequate to account for overall changes for core lengths more than 500 m. This suggests that the muon disc thicknesses of various EAS varied substantially.

The relative time distinction between average arrival times for muons and electrons rises as the distance from the shower core increases. The disparity between mean arrival times of the shower fronts increases from the initial value above $R = 1000$ m. The average arrival times are later as the energy level increases. Muons arrive before electrons over a core distance of $R = 500$ m which is true with the both energy values; the increase in the arrival time with increasing energy results from differing statistics regarding particle arrival time distribution. An EAS with higher energy has a larger spread of particle arrival times at long core distances for the specific particle type.

As evidenced by the thickening of the shower front with the primary energy, the tail seems to be more pronounced for EAS of higher than of lower energy.

This is because of the EAS's greater extension at higher energies. There is a discrepancy in the arrival time of muons and electrons with observation level because electromagnetic and muonic components have dissimilar shower development. On average, muons are formed higher in the atmosphere and are scattered considerably less than electrons, their descent trajectories are nearly straight lines.

Fig. 3 shows the simulated mean arrival time of e^-, e^+, and μ as a function of R using the AIRES program for three primary particles (protons, iron, and oxygen nuclei), at energies 10^{19} and 10^{20} eV with zenith angles 0°, 10°, and 20°. The dependence of the time profile of the shower disk on the zenith angle has been examined.

Additionally, for inclined showers, due to the electromagnetic component of a shower, at ground level, these particles dominate the signal everywhere, being produced by the disintegration of two neutral pions, which are absorbed at high altitudes in the atmosphere [2]. In contrast, the radial component of relative shower-to-shower variations appears to be more uniform and diminishes with increasing incident angle. This could result from higher path lengths for inclined showers, resulting in greater Coulomb scattering of electrons. The number of muons in EAS determined from PAO data is 1.5 to 2.2 times greater than expected in calculations. The precise difference is determined by the zenith angle (see analytic approach [24]).

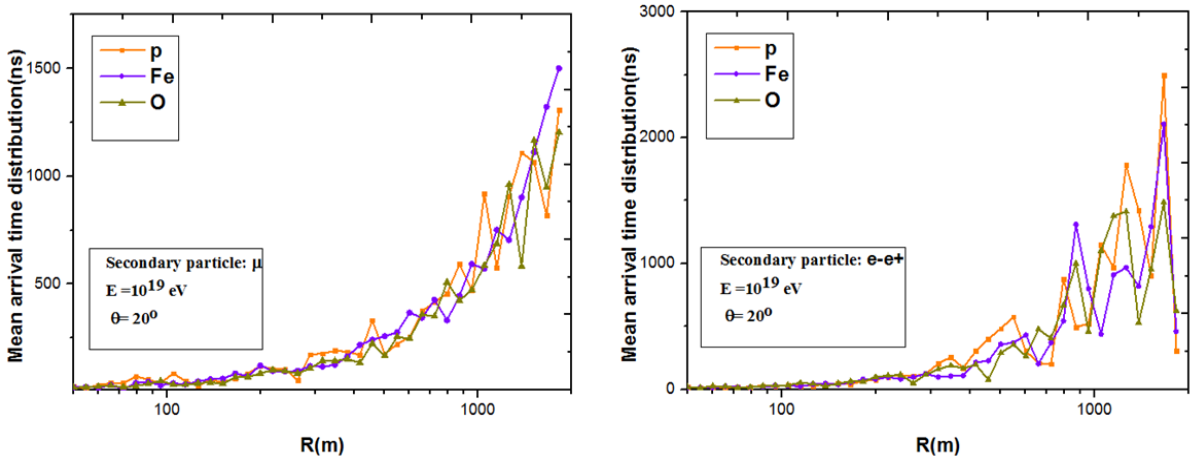

Fig. 4. Mean arrival time of electron-positron and muon for primary particles p, Fe, and O with primary energy 10^{19} eV for inclined showers. (See color Figure on the journal website.)

Fig. 4 shows the mean arrival time of e^-, e^+, and μ for primary particles p, Fe, and O at the primary energy 10^{19} eV with a fixed zenith angle. It can be seen that there is no discernible difference in the shower time profiles of the three primary particles. A qualitative comparison makes it clear that the distribution of the proton primary is fuzzier as the shower front thickness increases at almost all core distances. This Figure illustrates intra-shower oscillations in arrival times, with the proton primary showing more significant fluctuations than other primaries.

4.1. Mean arrival time parameterization

One can directly examine the behavior of the parameters of the fitting functions or, even better, the behavior of empirically quantifiable pulse shape pa-

rameters that can be specified in terms of the function parameters. To describe the behavior of the mean arrival time, a parameterized formula was obtained for mean arrival time distributions with a distance range 0 - 1500 m from the shower axis by fitting the Monte Carlo simulation results to a polynomial:

$$\tau(R) = K_0 + K_1 R + K_2 R^2 + K_3 R^3, \qquad (5)$$

where $\tau(R)$ is the mean arrival time of e^-, e^+, and μ, R is the distance of secondary particles from the shower core with a range 0 - 1500 m, and K_0, K_1, K_2, and K_3 are coefficients that depend on the primary and secondary particles produced by EAS. The values obtained for these coefficients are shown in the Table.

Coefficients of polynomial function Eq. (5) obtained to parameterize of AIRES simulation for p, ^{56}Fe, and ^{16}O primary particles at the energy 10^{19} eV at vertical EAS

Primary particles	Secondary particles	Coefficients $E = 10^{19}$, θ = 0				R^2	SD
		K_0	K_1	K_2	K_3		
p	e^-e^+	15411.3	−29789.3	21560.4	−6941.6	0.922	600.6
	μ	25923.2	−46528.5	31104.6	−9203.8	0.985	398.5
^{56}Fe	e^-e^+	28950.8	−53405.5	36778.5	−11233.5	0.955	605.3
	μ	14139.2	−26414.9	18437.8	−5713.8	0.994	389.7
^{16}O	e^-e^+	−39109.4	66359.0	−41159.7	10993.8	0.928	532.9
	μ	3066.5	−6913.0	5747.7	−2103.0	0.995	410.5

Fig. 5 shows the results of mean arrival time simulated using the AIRES system (symbols) compared with the results obtained using Eq. (5) (solid line) for e^-, e^+, and μ secondary particles, which were initiated by p, ^{56}Fe, and ^{16}O primaries at 10^{19} eV in a vertical shower.

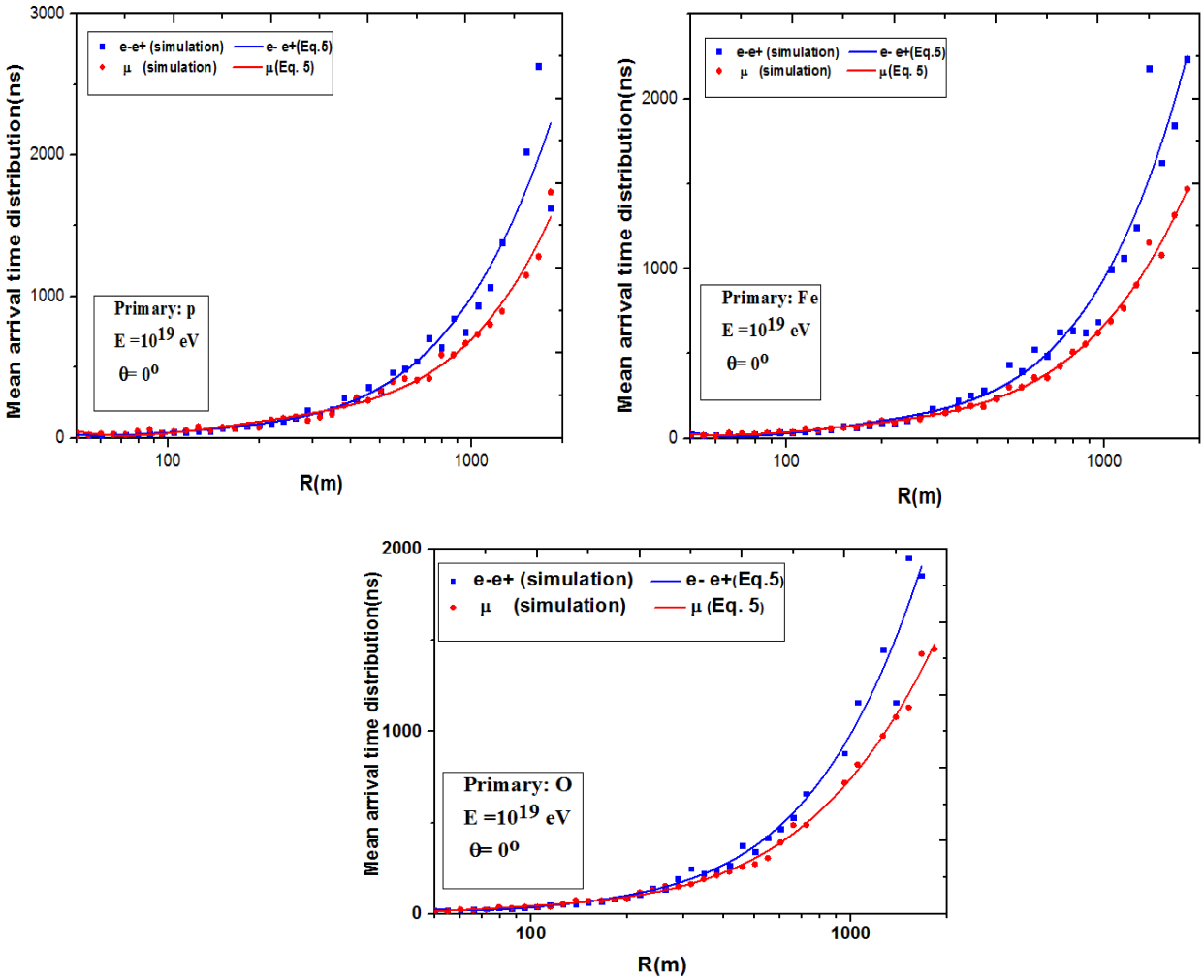

Fig. 5. Mean arrival time distribution simulated with AIRES (symbols) compared with the results obtained using Eq. (5) (solid lines) for p, ^{56}Fe, and ^{16}O primaries with energy 10^{19} eV in vertical showers. (See color Figure on the journal website.)

4.2. Comparative analysis of the experimental data produced by the KASCADE-Grande experiment and Sciutto's simulations

EASs initiated with primary cosmic ray particles at energy between 100 TeV and 1 EeV were measured by the KASCADE-Grande experiment [25], which combined a Piccolo trigger array, a Grande detector array, and an original KASCADE experiment [26].

Fig. 6, *a* shows the parameterized mean arrival time distribution obtained using Eq. (5) (dashed lines) compared with the experimental results from KASCADE (solid lines) [27]. In this Figure, a proton might initiate an EAS with energy 10^{20} eV. The parameterized form of a shower front used in the reconstruction of the direction of the shower differs from its true form, according to the simulations, which causes a difference between the actual and estimated arrival timings of the shower core. This discrepancy is quantified in terms of the size of the electron shower.

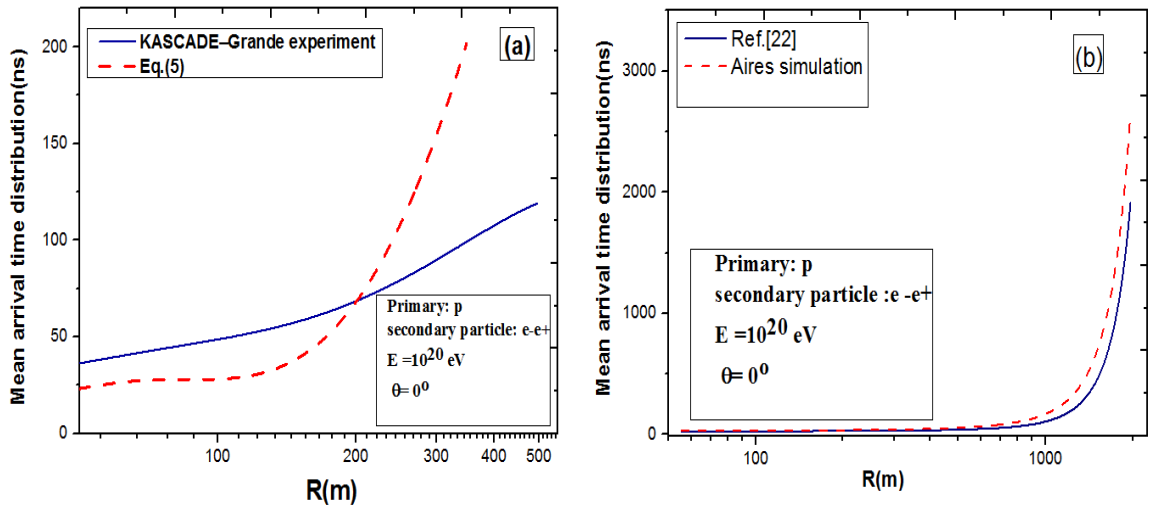

Fig. 6. *a* – Comparison of the parameterized mean arrival time distribution obtained using Eq. (5) with the experimental results from KASCADE for a primary proton at energy 10^{16} eV in vertical EAS for e^- and e^+ secondary particles. *b* – Comparison of the parameterized mean arrival time distribution obtained using Eq. (5) from the AIRES simulations (dash line) and Ref. [22] (solid line), for a primary proton at energy 10^{20} eV. (See color Figure on the journal website.)

Fig. 6, *b* contrasts AIRES simulation results with the mean arrival time data from [22] (solid line). This Figure demonstrates good agreement between the results of [22] and AIRES simulation of the e^- and e^+ secondary particles initiated by a proton at 10^{20} eV in a vertical EAS $\theta = 0°$.

5. Conclusion

To investigate the difference between the dependence of the muonic and electromagnetic components' arrival times on core distance, the mean arrival time and its variance distributions were used to estimate the typical time profile of muonic and electromagnetic shower disks. With distances $R > 1000$ m from a core, the muonic component often reaches the ground before the electromagnetic component; this is because of the additional path length and geometrical delays due to the muons' sub-luminal velocity.

In addition, a polynomial parameterization equation was established for a $R < 1500$ m distance range from the axis of a shower in vertical showers. This can be used to determine the mean arrival time distribution for various secondary particles with ultra-high primary energies (10^{19} - 10^{20} eV). It has been validated against simulations performed with the AIRES system.

For the majority of relevant distances and all zenith angles, the obtained results agree with those obtained by direct simulations sufficiently well to be useful for practical applications.

The authors thank Mustansiriyah University in Baghdad, Iraq and AIRES system creators for their support in this work.

REFERENCES

1. J.S. Pryga et al. Analysis of the capability of detection of extensive air showers by simple scintillator detectors. Universe 8 (2022) 425.
2. A.A. Al-Rubaiee, H.A. Jassim, I. Al-Alawy. Modulating the lateral profile in extensive air showers for Yakutsk EAS array. J. Astrophys. Astron. 42 (2021) 52.
3. P. Sokolsky, G. Thomson. *Introduction to Ultra High Energy Cosmic Ray Physics*. 2nd ed. (Taylor & Francis Group, LLC, 2020) 174 p.

4. R. Haeusler et al. Distortions of experimental muon arrival time distributions of extensive air showers by the observation conditions. Astropart. Phys. 17 (2002) 421.
5. S.J. Sciutto. The AIRES system for air shower simulations. An update. arXiv: astro-ph/0106044v1 (2001).
6. I.F. Hussein, A.A. Al-Rubaiee. Estimating the longitudinal development of atmospheric cascades at high energies. AIP Conf. Proc. 2591 (2023) 030072.
7. P. Bassi, G. Clark, B. Rossi. Distribution of arrival times of air shower particles. Phys. Rev. 92 (1953) 441.
8. H. Nogima. Development and status of the Pierre Auger Observatory. Braz. J. Phys. 32(4) (2002) 895.
9. Pierre Auger Collaboration. Proceedings of the 29th International Cosmic Ray Conference (ICRC 2005), Pune, India, August 3 - 10, 2005 (Mumbai: Tata Institute of Fundamental Research, 2005).
10. T. Antoni et al. Time structure of the extensive air shower muon component measured by the KASCADE experiment. Astropart. Phys. 15(2) (2001) 149.
11. T. Antoni et al. The information from muon arrival time distributions of high-energy EAS as measured with the KASCADE detector. Astropart. Phys. 18 (2003) 319.
12. M. Ambrosio et al. Time structure of individual extensive air showers. Astropart. Phys. 11 (1999) 437.
13. N. Inoue et al. Arrival-time distribution of air-shower electrons near the core. J. Phys. G 15 (1989) 1899.
14. W.E. Hazen, H.Y. Dai, E.S. Hazen. Study of a mini-array for the Linsley effect in cosmic-ray air showers. J. Phys. G 15 (1989) 113.
15. P.K.F. Grieder. *Extensive Air Showers. High Energy Phenomena and Astrophysical Aspects – A Tutorial, Reference Manual and Data Book*. Vol. I (Berlin Heidelberg, Springer-Verlag, 2010) 1118 p.
16. C.P. Woidneck, E. Bohm. The longitudinal particle distribution in the extensive air shower disc. J. Phys. A 8 (1975) 997.
17. E.J. de Villiers et al. The arrival time distribution of muons in extensive air showers. J. Phys. G 12 (1986) 547.
18. M. Agnetta et al. Time structure of the extensive air shower front. Astropart. Phys. 6 (1997) 301.
19. M. Ambrosio et al. Interpretation of the time structure of the EAS disc measured by the GREX/COVER_PLASTEX experiment. Astropart. Phys. 7 (1997) 329.
20. S. Sciutto. AIRES. User's Manual and reference guide. Version 2.8.4a (2006).
21. S. Sciutto. AIRES: A System for Air Shower Simulations. User's guide and reference manual. Version 2.2.0 (1999).
22. S.J. Sciutto. AIRES. User's manual and reference guide. Version 2.6.0 (La Plata, Argentina, 2002).
23. S.J. Sciutto. AIRES: a System for Air Shower Simulations. User's guide and reference manual. Version 19.04.00 (2019).
24. L. Nellen (for the Pierre Auger Collaboration) The observation of a muon deficit in simulations from data of the Pierre Auger Observatory. J. Phys.: Conf. Ser. 409 (2013) 012107.
25. G. Navarra et al. KASCADE-Grande: a large acceptance, high-resolution cosmic-ray detector up to 10^{18} eV. Nucl. Instrum. Methods A 518 (2004) 207.
26. T. Antoni et al. The cosmic-ray experiment KASCADE. Nucl. Instrum. Methods A 513 (2003) 490.
27. W.D. Apel et al. Time structure of the EAS electron and muon components measured by the KASCADE-Grande experiment. Astropart. Phys. 29 (2008) 317.

І. Ф. Хусейн[1,*], А. А. Аль-Рубаї[1], А. Ф. Мхайбер[2]

[1] *Університет Мустансірія, науковий коледж, фізичний факультет, Багдад, Ірак*
[2] *Багдадський університет, педагогічний коледж природничих наук, фізичний факультет, Багдад, Ірак*

*Відповідальний автор: itabfadhil@uomustansiriyah.edu.iq

РОЗПОДІЛ СЕРЕДНЬОГО ЧАСУ ПРИБУТТЯ ШИРОКИХ АТМОСФЕРНИХ ЗЛИВ ПРИ НАДВИСОКИХ ЕНЕРГІЯХ

У статті досліджуються широкі атмосферні зливи через оцінку розподілу середнього часу прибуття мюонів і електронів при надвисоких енергіях для різних частинок космічних променів. Пакет Монте-Карло AIRES (версія 19.04.00) використовувався для виконання моделювання при енергіях 10^{19} і 10^{20} еВ. Було досліджено вплив первинних частинок (p, ^{56}Fe і ^{16}O), енергій і зенітних кутів (0°, 10° і 20°) на середній час приходу мюонних і електромагнітних компонент, утворених у широкій атмосферній зливі. Розраховано параметризовані середні розподіли часу прибуття для вторинних частинок e^-, e^+ та μ, створених протонами та ядрами заліза і кисню при енергії 10^{19} еВ у вертикальній зливі. Поліноміальна функція для часових розподілів у вертикальних зливах була встановлена з використанням результатів цього моделювання. Результати порівнювалися з експериментом KASCADE-Grande та моделюванням Шутто при енергії 10^{20} еВ і $\theta = 0$. У цій роботі побудова бази даних, що може бути використана для обчислення часу прибуття елементарних частинок надвисоких енергій, і аналітичний опис залежності часу прибуття від відстані мали вирішальне значення.

Ключові слова: середній розподіл часу прибуття, широка атмосферна злива, AIRES, моделювання електромагнітної зливи.

Надійшла / Received 07.06.2024